Case of equilibrium beam distribution dependence on storage ring nonlinearity

Jingyi Tang[1,2] and Xiaobiao Huang[2,*]

[1]*Department of Applied Physics, Stanford University, Stanford, California 94305, USA*
[2]*SLAC National Accelerator Laboratory, 2575 Sand Hill Road, Menlo Park, California 94025, USA*

(Received 11 March 2022; accepted 27 June 2022; published 6 July 2022)

In an electron storage ring, the emittances are determined by the beam energy and the linear lattice; the effects of lattice nonlinearity are usually negligible. In this study, we show a case where the vertical emittance has a strong quadratic dependence on the vertical chromaticity, a form of lattice nonlinearity. In this case, a crab cavity is present in the lattice, which couples the longitudinal and vertical motions of the beam. A theoretic analysis is conducted to derive the emittance dependence on chromaticity, using the normal form approach to decouple the longitudinal and vertical motion. Particle tracking simulations are performed to verify the analytic results and a good agreement is found. The dependence of equilibrium emittances on nonlinear lattice properties as demonstrated in this paper may provide new possibilities for design options and machine control.

DOI: 10.1103/PhysRevAccelBeams.25.074002

I. INTRODUCTION

Particles in a storage ring oscillate around the reference orbit in three directions (x, y, and s). Typically the three degrees of freedom are only weakly coupled, and hence the motion in each plane can be separately described. The distribution of a particle beam in a transverse plane is often characterized by the emittance, which represents the phase space area occupied by the beam, in (x, p_x) or (y, p_y) coordinates. The emittances are important measures of the beam quality as they are closely related to the performances of the beam applications, for example, in terms of luminosity in colliders and photon beam brightness in light sources.

Emittances in an electron storage ring are given by the equilibrium state of the quantum diffusion and radiation damping processes, both of which are consequences of photon emissions in the bending fields. As a consequence of the many small stochastic excitations, the electron beam distributions acquire a Gaussian distribution in the six-dimensional phase space. Since the excitation of the betatron motion through photon emission depends on the Courant-Snyder optics functions and the dispersion functions in the bending fields [1], which in turn are given by the linear lattice, the beam emittances in an electron storage ring are determined by the beam energy and the linear lattice.

In a typical case of small linear coupling between the two transverse planes, the horizontal emittance and the energy spread can be calculated analytically by evaluating the radiation integrals, using linear lattice functions (beta functions and dispersion functions [1]), along with the distribution of bending fields [2]. In the case of linearly coupled motion, the equilibrium distribution can be computed numerically with the lattice model [3,4], which accounts for the distribution of bending fields and focusing gradients around the closed orbit of the beam. In all existing machines, the vertical emittance is determined by the level of horizontal-vertical linear coupling and the distribution of vertical dispersion functions in the bending fields. Although nonlinear magnets, such as sextupoles, affect the linear lattice functions through the magnetic feed-down effects, the nonlinearity in the dynamics around the closed orbit is negligible in the determination of the equilibrium distribution for a typical electron storage ring. In short, the equilibrium beam distribution in a typical electron storage ring is given by the linear lattice.

In this study, we report an interesting case in which the vertical emittance shows a strong dependence on the vertical chromaticity. This case comes from the study of short pulse generation with transverse deflecting cavities (a.k.a., crab cavities) in the SPEAR3 storage rings [5–7]. In a previous study, it was found that the tilted distribution in the vertical-longitudinal planes in the bending fields causes an excitation of the vertical emittance [7]. Because the tilted distribution is the consequence of the linear coupling between the two planes, this emittance excitation mechanism is still of the nature of linear motion. The chromaticity is a measure of the

*xiahuang@slac.stanford.edu

dependence of the betatron tune (i.e., the number of betatron oscillations per revolution) on the momentum deviation of a particle. A nonzero vertical chromaticity introduces nonlinear coupling between the y and s planes and in turn alters the excitation of the vertical emittance by crab cavities.

We conducted an analytic study to investigate the dependence of vertical emittance on the vertical chromaticity of a storage ring with crab cavities. This is done by calculating the excitation of the decoupled normal modes by photon emissions. The normal form approach is applied to obtain the nonlinear transformation between the usual phase space coordinates and the decoupled normal mode coordinates. Through the analysis, we derived an expression of the vertical emittance in electron storage rings with crab cavities, which explicitly demonstrates the quadratic dependence on the vertical chromaticity. Simulation studies, using simplified or full lattice models, are conducted to verify the analysis.

This paper is organized as follows: In Sec. II, we will present the theoretic analysis. Section III shows the simulation results. The conclusion is given in Sec. IV.

II. THEORETIC ANALYSIS

With three degrees of freedom, the beam motion can be decomposed into three eigenmodes (also referred to as normal modes). The emittances defined for the eigenmodes, or eigenemittances, are preserved quantities through symplectic transport and thus true measures of the beam quality. During photon emission by synchrotron radiation, an electron loses an energy quantum within a finite formation length much shorter than the periods of betatron and synchrotron oscillations, resulting in a change in its momentum deviation coordinate. Because of the coupled motion, a change in momentum coordinate may correspond to a shift in phase space that spans all three eigenmodes. The excitation of the eigenemittances can be computed by projecting this shift to the eigenmodes, using the transformation between the usual Frenet-Serret coordinates and the eigenmode coordinates.

For linearly coupled motion, the decoupling transformation between the usual coordinates and the eigenmode coordinates can be determined by diagonalizing the transfer matrix. When there is nonlinear coupling, the motion can still be decoupled into three normal modes. In general, the transformation between the usual coordinates and the normal mode coordinates will also be nonlinear. The nonlinear transformation to the normal modes can be found with the normal form methods [8].

A. Decoupling of linear motion with crab cavity

We consider the excitation of vertical emittance in a storage ring with crab cavities as in Ref. [7]. For simplicity, a single crab cavity is assumed in the storage ring, with the coupling strength given by

$$\chi = \frac{eVk}{E}, \tag{1}$$

where V is the deflecting voltage, $k = \omega/c$ is the angular wave number, ω is the angular frequency of the crab cavity, and E is the beam energy. Assuming the crab cavity location is free of horizontal dispersion and the $x-y$ coupling is weak, we can ignore the horizontal motion in this analysis. The phase space coordinates of a particle in the vertical-longitudinal planes are $\mathbf{X} = (y, p_y, z, \delta)^T$, where ^{T} stands for the transpose of a vector or matrix.

The coupled linear motion of the particle observed at a given location is represented by the one-turn transfer matrix of the phase space coordinates. Suppose the one-turn transfer matrix for $\mathbf{X}$ is

$$\mathbf{T} = \begin{pmatrix} \mathbf{M} & \mathbf{m} \\ \mathbf{n} & \mathbf{N} \end{pmatrix}, \tag{2}$$

where the sub-blocks are all 2×2 matrices, the decoupling transformation is [9],

$$\mathbf{X}_a = \mathbf{V}^{-1}\mathbf{X}, \qquad \mathbf{V} = \begin{pmatrix} r\mathbf{I} & \mathbf{C} \\ -\mathbf{C}^+ & r\mathbf{I} \end{pmatrix}, \tag{3}$$

where $\mathbf{C}^+$ is the symplectic conjugate of matrix $\mathbf{C}$. The decoupled coordinates are $\mathbf{X}_a = (y_a, p_{y_a}, z_b, p_{z_b})^T$, $r = \sqrt{1 - ||\mathbf{C}||}$, and

$$\mathbf{C} = \frac{-\mathbf{H}\,\mathrm{sgn}(\mathrm{Tr}[\mathbf{M}-\mathbf{N}])}{r\sqrt{(\mathrm{Tr}[\mathbf{M}-\mathbf{N}])^2 + 4||\mathbf{H}||}}, \tag{4}$$

where $\mathbf{H} \equiv \mathbf{m} + \mathbf{n}^+$ and $\mathrm{sgn}(\cdot)$ stands for the sign of its argument. Reference [7] gave formulas for the elements of matrix $\mathbf{C}$ to the first order in χ.

Similar to the betatron coordinates in the uncoupled case, the decoupled coordinates can be normalized via a coordinate transformation, with

$$\begin{pmatrix} \bar{y}_a \\ \bar{p}_{y_a} \end{pmatrix} = \mathbf{A}_y^{-1} \begin{pmatrix} y_a \\ p_{y_a} \end{pmatrix}, \qquad \begin{pmatrix} \bar{z}_b \\ \bar{p}_{z_b} \end{pmatrix} = \mathbf{A}_z^{-1} \begin{pmatrix} z_b \\ p_{z_b} \end{pmatrix}, \tag{5}$$

where

$$\mathbf{A}_y = \begin{pmatrix} \sqrt{\beta_y} & 0 \\ -\frac{\alpha_y}{\sqrt{\beta_y}} & \frac{1}{\sqrt{\beta_y}} \end{pmatrix}, \quad \mathbf{A}_z = \begin{pmatrix} \sqrt{\beta_z} & 0 \\ -\frac{\alpha_z}{\sqrt{\beta_z}} & \frac{1}{\sqrt{\beta_z}} \end{pmatrix}, \tag{6}$$

and $\beta_{y,z}$ and $\alpha_{y,z}$ are vertical and longitudinal Courant-Snyder parameters, respectively. To the first order of χ, the Courant-Snyder parameters for the decoupled coordinates are the same as their uncoupled counterparts. The action variables of the decoupled coordinates are given by

$$\bar{J}_y = \frac{1}{2}(\bar{y}_a^2 + \bar{p}_{y_a}^2), \qquad \bar{J}_z = \frac{1}{2}(\bar{z}_b^2 + \bar{p}_{z_b}^2). \tag{7}$$

The decoupled and normalized coordinates, $\bar{\mathbf{X}}_a = (\bar{y}_a, \bar{p}_{y_a}, \bar{z}_b, \bar{p}_{z_b})^T$, are related to the original phase space coordinates through

$$\bar{\mathbf{X}}_a = \mathbf{A}^{-1}\mathbf{V}^{-1}\mathbf{X}, \tag{8}$$

with

$$\mathbf{A} = \begin{pmatrix} \mathbf{A}_y & \mathbf{0} \\ \mathbf{0} & \mathbf{A}_z \end{pmatrix}. \tag{9}$$

B. Quantum excitation for coupled linear motion

When an electron emits a photon in a storage ring, the excitation in the original coordinates is $\Delta\mathbf{X} = \boldsymbol{\xi} = (0, 0, 0, -u)^T$, where u is the energy of the photon. The excitation to the normalized coordinates is thus

$$\Delta\bar{\mathbf{X}}_a = \mathbf{A}^{-1}\mathbf{V}^{-1}\boldsymbol{\xi} = (-u)\begin{pmatrix} -\frac{C_{12}}{\sqrt{\beta_y}} \\ -\frac{\alpha_y C_{12} + \beta_y C_{22}}{\sqrt{\beta_y}} \\ 0 \\ r\sqrt{\beta_z} \end{pmatrix}, \tag{10}$$

from which we obtain the quadratic terms in the changes to the action variables

$$\Delta J_y = \frac{u^2}{2\beta_y}(C_{12}^2 + (\alpha_y C_{12} + \beta_y C_{22})^2), \tag{11}$$

$$\Delta J_z = \frac{r^2 u^2 \beta_z}{2}. \tag{12}$$

Equation (11) reproduces the result in Eqs. (74)–(75) of Ref. [7]. Integrating all photon emissions around the ring and considering radiation damping, one can derive the vertical emittance due to linear coupling by the crab cavity.

Equation (12) gives the excitation to the longitudinal action. To the first order of the coupling strength, χ, the crab cavity has no impact on the longitudinal excitation. Following the same derivation, as was done in Ref. [2], the longitudinal equilibrium emittance can be derived to give

$$\epsilon_z = C_q \gamma^2 \frac{\langle \beta_z / |\rho|^3 \rangle}{\mathcal{J}_z \langle 1/\rho^2 \rangle}, \tag{13}$$

where $\mathcal{J}_z$ is the longitudinal damping partition. Equation (13) agrees with the usual formula for equilibrium momentum spread for the weak longitudinal focusing cases [2]. However, it also applies to the longitudinal strong focusing case where β_z can substantially vary around the ring.

C. Quantum excitation of nonlinearly coupled motion

In the general case when the beam motion is nonlinear and coupled between the two planes, the one-turn map (for the usual coordinates $\mathbf{X}$) can be represented by a Lie map. The linear and nonlinear beam motion can be separated by expressing the Lie map as [10]

$$M = e^{:f_2:} e^{:f_{\text{non}}:}, \tag{14}$$

where f_2 is a quadratic polynomial and represents the linear motion and f_{non} contains higher order terms and represents the nonlinear motion. The decoupling coordinate transformation can also be separated into linear and nonlinear parts

$$\mathbf{X}_n = e^{:F:}\mathbf{X}, \qquad e^{:F:} = e^{:F_2:} e^{:F_{\text{non}}:}, \tag{15}$$

where $\mathbf{X}_n$ denotes the decoupled coordinates and F_2 and F_{non} are the generating functions for the linear and nonlinear parts of the transformation, respectively. The linear transformation can be found from the linear map $e^{:f_2:}$ with the eigenanalysis of the latter, or, for the two-dimensional case, with the procedure described in Ref. [9] and adopted here.

The nonlinear portion of the decoupling transformation can be found from the nonlinear map and the eigenbasis of the linear motion. Considering only the third order polynomials in the nonlinear motion, i.e., assuming $f_{\text{non}} = f_3$, with

$$f_3 = \sum_{a,b,c,d=0}^{3} C_{abcd}^{(3)} |abcd\rangle, \tag{16}$$

where $|abcd\rangle$ is an eigenvector of the linear map f_2,

$$:f_2:|abcd\rangle = i[(a-b)\mu_y + (c-d)\mu_z)]|abcd\rangle, \tag{17}$$

with integers a, b, c, and d that satisfy $a + b + c + d = 3$, $\mu_y = 2\pi\nu_y$, $\mu_z = 2\pi\nu_z$, and ν_y and ν_z are the vertical and longitudinal betatron tunes, respectively. The third order terms in F_{non} are given by [10]

$$F_3 = \sum_{\substack{a,b,c,d=0 \\ a\neq b \text{ or } c\neq d}}^{3} \frac{C_{abcd}^{(3)} |abcd\rangle}{1 - e^{i[(a-b)\mu_y + (c-d)\mu_z)]}} \tag{18}$$

D. Nonlinear coupled motion with crab cavity and chromaticity

Including the effect of vertical chromaticity, the Hamiltonian of beam motion in a ring with a crab cavity is

$$H = \mu_y J_y(y, p_y) + \mu_z J_z(z, \delta) + \chi \delta_D(\theta - \theta_0) yz + 2\pi\xi_y J_y(y, p_y)\delta, \tag{19}$$

where J_y and J_z are the uncoupled vertical and longitudinal action variables, respectively, ξ_y is the vertical chromaticity, $\delta_D(\cdot)$ is the Dirac delta function, and we are using $\theta = \frac{2\pi s}{C}$ as the free variable, with s being the path length and C, the circumference of the ring. The χ term represents the coupling effect by the crab cavity located at θ_0.

With normalized and linearly decoupled coordinates, the Hamiltonian becomes

$$H = \mu_y \bar{J}_y(\bar{y}_a, \bar{p}_{y_a}) + \mu_z \bar{J}_z(\bar{z}_b, \bar{p}_{z_b}) + 2\pi\xi_y J_y(y, p_y)\delta, \tag{20}$$

where y, p_y, and δ are connected to the decoupled coordinates through the linear transformation in Eq. (8) and we have omitted the small changes in the tunes due to the crab cavity.

The generating functions for the linear and nonlinear parts of the Lie map for the beam motion corresponding to the above Hamiltonian are $f_2 = -\mu_y \bar{J}_y - \mu_z \bar{J}_z$ and $f_3 = -2\pi\xi_y J_y \delta$, respectively.

To proceed, we first normalize the original phase space coordinates $\bar{\mathbf{X}} = (\bar{y}, \bar{p}_y, \bar{z}, \bar{p}_z)$, which can be transformed from $\mathbf{X}$ with Courant-Snyder parameters $\bar{\mathbf{X}} = \mathbf{A}^{-1}\mathbf{X}$. To the first order of χ, the Courant-Snyder parameters for the original coordinates are the same as their decoupled counterparts. Therefore, the normalized coordinates, before and after decoupling, are related through

$$\bar{\mathbf{X}}_a = \mathbf{A^{-1}V^{-1}A}\bar{\mathbf{X}} = \bar{\mathbf{V}}^{-1}\bar{\mathbf{X}}, \tag{21}$$

where the normalized decoupling matrix $\bar{\mathbf{V}}$ is related to $\mathbf{V}$ by

$$\bar{\mathbf{V}} = \mathbf{A^{-1}VA} = \begin{pmatrix} r\mathbf{I} & \bar{\mathbf{C}} \\ -\bar{\mathbf{C}}^{+} & r\mathbf{I} \end{pmatrix}, \tag{22}$$

whose off-diagonal submatrix $\bar{\mathbf{C}}$ is given by

$$\bar{\mathbf{C}} = A_y^{-1}\mathbf{C}A_z. \tag{23}$$

With the notations in Eqs. (21)–(23) and the approximation that $r \approx 1$, we can transform the normalized original coordinates $\bar{\mathbf{X}}$ to linearly decoupled and normalized coordinate $\bar{\mathbf{X}}_a$

$$\begin{aligned} \bar{y} &= \bar{y}_a + \bar{\mathbf{C}}_{11}\bar{z}_b + \bar{\mathbf{C}}_{12}\bar{p}_{z_b} \\ \bar{p}_y &= \bar{p}_{y_a} + \bar{\mathbf{C}}_{21}\bar{z}_b + \bar{\mathbf{C}}_{22}\bar{p}_{z_b} \\ \bar{p}_z &= \bar{p}_{z_b} + \bar{\mathbf{C}}_{21}\bar{y}_a - \bar{\mathbf{C}}_{11}\bar{p}_{y_a}. \end{aligned} \tag{24}$$

The nonlinear map f_3 can therefore be expressed with decoupled and normalized coordinate $\bar{X}$ as

$$\begin{aligned} f_3 &= -\pi\xi_y(\bar{y}^2 + \bar{p}_y^2)\delta \\ &\approx -\frac{\pi\xi_y}{\sqrt{\beta_z}}[(\bar{p}_{z_b} - \bar{\mathbf{C}}_{11}\bar{p}_{y_a} + \bar{\mathbf{C}}_{21}\bar{y}_a)(\bar{y}_a^2 + \bar{p}_{y_a}^2) \\ &\quad + 2(\bar{\mathbf{C}}_{11}\bar{p}_{z_b}\bar{y}_a\bar{z}_b + \bar{\mathbf{C}}_{12}\bar{p}_{z_b}^2\bar{y}_a \\ &\quad + \bar{\mathbf{C}}_{21}\bar{p}_{z_b}\bar{p}_{y_a}\bar{z}_b + \bar{\mathbf{C}}_{22}\bar{p}_{z_b}^2\bar{p}_{y_a})], \end{aligned} \tag{25}$$

where we only keep the terms to the first order of the elements of $\bar{\mathbf{C}}$. Using Eq. (18), we obtain the generating function for the nonlinear transformation,

$$\begin{aligned} F_3 = \frac{-\pi\xi_y}{\sqrt{\beta_z}}\Big[&A_1\bar{p}_{y_a}\bar{p}_{z_b}\bar{z}_b + A_2\bar{y}_a\bar{p}_{z_b}\bar{z}_b \\ &+ A_3\bar{y}_a\bar{p}_{z_b}^2 + A_4\bar{p}_{y_a}\bar{p}_{z_b}^2 \\ &+ A_5\bar{p}_{y_a}\bar{z}_b^2 + A_6\bar{y}_a\bar{z}_b^2 \\ &+ \frac{1}{2}\left(\bar{p}_{z_b} + \bar{z}_b\cot\frac{\mu_z}{2}\right)(\bar{y}_a^2 + \bar{p}_{y_a}^2)\Big], \end{aligned} \tag{26}$$

where A_i, $i = 1$–6, are functions of the elements in matrix $\bar{\mathbf{C}}$ and the betatron phase advances,

$$\begin{aligned} A_1 &= \bar{\mathbf{C}}_{21} + \frac{\bar{\mathbf{C}}_{11}\sin\mu_y + \bar{\mathbf{C}}_{22}\sin(2\mu_z)}{\cos\mu_y - \cos(2\mu_z)} \\ A_2 &= \bar{\mathbf{C}}_{11} + \frac{-\bar{\mathbf{C}}_{21}\sin\mu_y + \bar{\mathbf{C}}_{12}\sin(2\mu_z)}{\cos\mu_y - \cos(2\mu_z)} \\ A_3 &= \bar{\mathbf{C}}_{12} + \frac{1}{2}\bar{\mathbf{C}}_{22}\cot(\mu_y/2) \\ &\quad - \frac{1}{2}\frac{\bar{\mathbf{C}}_{22}\sin\mu_y + \bar{\mathbf{C}}_{11}\sin(2\mu_z)}{\cos\mu_y - \cos(2\mu_z)} \\ A_4 &= \bar{\mathbf{C}}_{22} - \frac{1}{2}\bar{\mathbf{C}}_{12}\cot(\mu_y/2) \\ &\quad + \frac{1}{2}\frac{\bar{\mathbf{C}}_{12}\sin\mu_y - \bar{\mathbf{C}}_{21}\sin(2\mu_z)}{\cos\mu_y - \cos(2\mu_z)} \\ A_5 &= \frac{1}{2}\frac{\bar{\mathbf{C}}_{21}\sin(2\mu_z) - 2\bar{\mathbf{C}}_{12}\cot(\mu_y/2)\sin^2\mu_z}{\cos\mu_y - \cos(2\mu_z)} \\ A_6 &= \frac{1}{2}\frac{\bar{\mathbf{C}}_{11}\sin(2\mu_z) + 2\bar{\mathbf{C}}_{22}\cot(\mu_y/2)\sin^2\mu_z}{\cos\mu_y - \cos(2\mu_z)}. \end{aligned} \tag{27}$$

It is worth noting that when $\mu_y \approx 2\mu_z$, the small denominators in Eq. (27) lead to divergence. This signifies a nonlinear resonance condition for which our perturbation

approach breaks down. In practice, such a condition is to be avoided to prevent the beam from blowing up.

The nonlinearly decoupled coordinates, or normal coordinates $\mathbf{X_n} = (y_n, p_{y_n}, z_n, p_{z_n})^T$, can be obtained by applying the nonlinear transformation to the linearly decoupled coordinates, i.e., with

$$y_n = e^{:F_3:}\bar{y}_a, \qquad p_{y_n} = e^{:F_3:}\bar{p}_{y_a}, \quad \text{etc.} \tag{28}$$

Considering an electron with an initial energy deviation δ and longitudinal position z that emits a photon of energy u, we can derive the quadratic terms in the changes to the action variables for the (y_n, p_{y_n}) plane, $J_{y_n} = \frac{1}{2}(y_n^2 + p_{y_n}^2)$, which are found to be

$$\begin{aligned}\Delta J_{y_n} &= \frac{1}{2}\beta_z(\bar{\mathbf{C}}_{12}^2 + \bar{\mathbf{C}}_{22}^2)u^2 + \frac{1}{2}\xi_y^2(f_z z^2 + f_\delta \delta^2)u^2 \\ &= \frac{1}{2}\mathcal{H}_c u^2,\end{aligned} \tag{29}$$

where f_z and f_δ are functions of A_i representing the nonlinear coupling. The first term on the right hand of Eq. (29) is the emittance from linear coupling and is consistent with the results in Eq. (11). The second term shows the effects of nonlinear coupling, which increases quadratically with the vertical chromaticity ξ_y. By integrating all emitted photons, the vertical emittance of a beam with nonlinear coupling by crab cavities and vertical chromaticity is found to be

$$\epsilon_y = C_q \frac{\gamma^2\langle\mathcal{H}_c\rangle}{\mathcal{J}_y\rho} = \frac{\mathcal{J}_z\langle\mathcal{H}_c\rangle\sigma_\delta^2}{\mathcal{J}_y}. \tag{30}$$

III. PARTICLE TRACKING SIMULATION

A. A simplified case

The emittance dependence on chromaticity derived in the above can be verified with particle tracking simulations. A simplified model is first considered. The model consists of an element representing the ring lattice with vertical chromaticity, a radio-frequency (rf) cavity element, a crab cavity, and a radiation element at which the damping and quantum excitation are applied to the particle coordinates. The ring lattice is implemented with a one-turn transfer matrix but with tune dependence on the momentum deviation coordinate. The parameters of the lattice used in the simulation are listed in Table I. Because the radiation effect is modeled with a single, discrete element, the matrix $\bar{\mathbf{C}}$ is simplified as

$$\bar{\mathbf{C}} = -\frac{1}{2}\chi\sqrt{\beta_y\beta_z}\begin{pmatrix} \frac{\sin\mu_y}{\cos\mu_y - \cos\mu_z} & 0 \\ 1 & \frac{\sin\mu_z}{\cos\mu_y - \cos\mu_z} \end{pmatrix} \tag{31}$$

TABLE I. Parameters of simplified model.

Parameters	Value	Unit
Energy	3	GeV
Crab cavity voltage V_d	2	MV
Crab cavity frequency f_{cb}	2857.8	MHz
rf frequency f_{rf}	476.3	MHz
Momentum compaction α_c	1.18×10^{-3}	
Scaled momentum compaction $\bar{\eta}$	0.2763	m
Beta functions β_y, β_z	2.5, 5.1	m
Momentum spread σ_δ	9.5×10^{-4}	
Longitudinal partition $\mathcal{J}_z$	1.697	
Synchrotron tune ν_s	0.010	

Correspondingly the calculation of $\langle\mathcal{H}_c\rangle$ for this model is relatively simple, yielding

$$\begin{aligned}\langle\mathcal{H}_c\rangle = &\frac{\beta_y\chi^2\bar{\eta}^2}{16}\csc^4\pi\nu_y \\ &+ \xi_y^2\frac{\beta_y\chi^2\pi^2\sigma_\delta^2}{8}(2\beta_z^2 - 15\bar{\eta}^2 + 17\bar{\eta}^2\csc^2\pi\nu_y)\csc^4\pi\nu_y.\end{aligned} \tag{32}$$

The first term in Eq. (32) is the linear term originated from the linear coupling by the crab cavity as found in Ref. [7], although in a different form corresponding to the simple model. The second term comes from the nonlinear coupling effect due to the vertical chromaticity and is simplified using the approximation $\sigma_z \approx \beta_z\sigma_\delta$.

About 1000 particles are tracked with the simplified model until the beam reached an equilibrium distribution, from which the vertical emittance is calculated. The simulation results are shown in Fig. 1. There is a good agreement between the simulation and the theory.

The key result in the derivation is the decoupling transformation, Eq. (26), which can be validated directly. This is done by tracking one off-energy particle with the

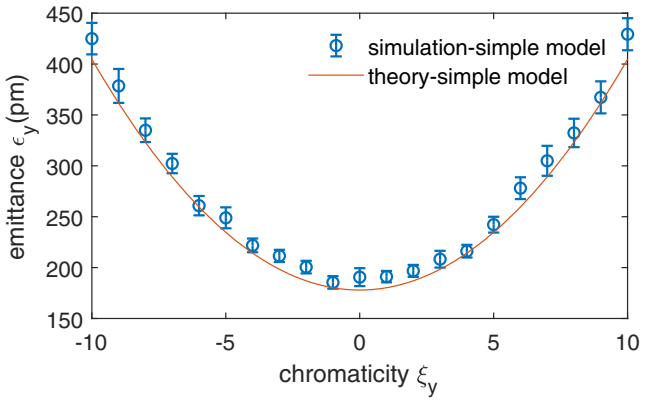

FIG. 1. Vertical emittance as a function of vertical chromaticity at vertical tune $\nu_y = 6.22$ for the simple model, simulation compared to theory.

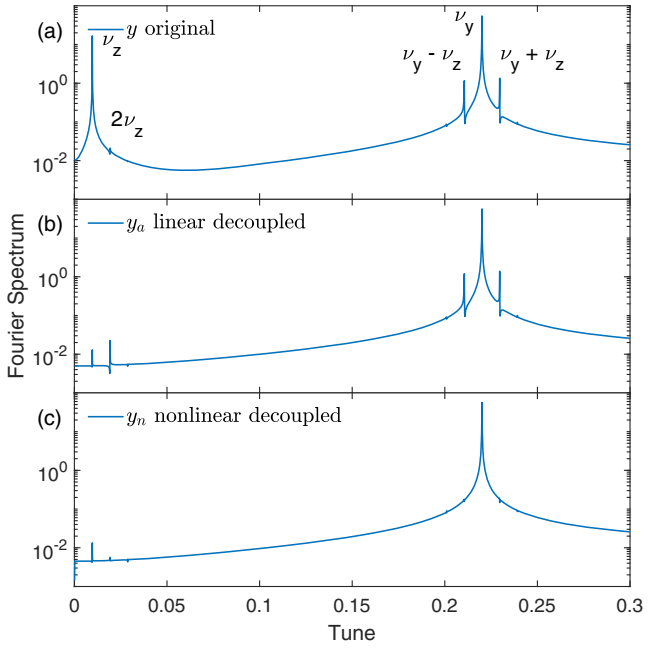

FIG. 2. Decoupling of the vertical turn-by-turn trajectory for a case with $\nu_y = 6.22$ and $\xi_y = 10$. The Fourier spectra for three coordinates, the original y (a), the linearly decoupled $\bar{y}_a$ (b), and the nonlinearly decoupled coordinates y_n (c), are shown. The resonance tune lines are labeled. The launching condition for tracking is $y = 10$ μm and $\delta = 1 \times 10^{-5}$.

radiation element turned off. We performed Fourier transform on the original coordinate y, linearly decoupled coordinate $\bar{y}_a$, and nonlinearly decoupled coordinate y_n and analyzed their frequency components, respectively. The spectra for the three coordinates are shown in Fig. 2. The y spectrum shows the two synchrotron sidebands besides the ν_y tune line, as well as a strong synchrotron component at ν_z. After the linear decoupling, the peak at ν_z disappears. However, the two synchrotron sideband peaks at $\nu_y + \nu_z$ and $\nu_y - \nu_z$ remain. A peak at $2\nu_z$ is also manifested. Those side peaks arise from the nonlinear coupling due to chromaticity. By applying the nonlinear transformation, all three side peaks are suppressed. This clearly shows the validity of the nonlinear decoupling transformation.

B. Simulation on SPEAR3 lattice

Particle tracking with a full ring model has also been conducted to verify the theory, using the SPEAR3 storage ring achromatic lattice and the tracking code ACCELERATOR TOOLBOX [11], with a setup similar to Ref. [7]. The particles are tracked for 30,000 turns when the equilibrium distribution is reached. When applying the theory to calculate the vertical emittance, integration over all bending magnets is needed. For simplicity, we assume that the synchrotron phase advance is linearly proportional to the distance traveled in bending magnets. The expression of vertical emittance in a real ring is given by

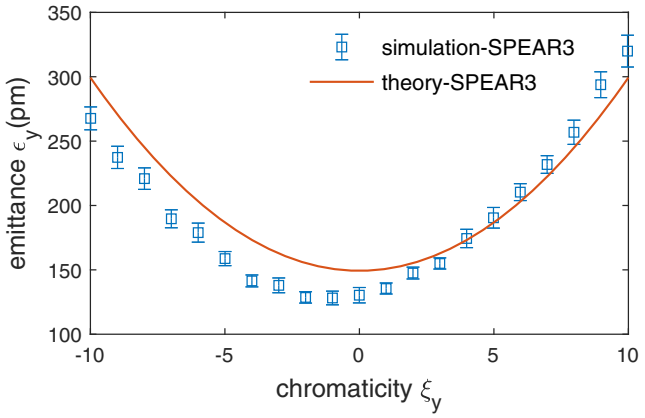

FIG. 3. Vertical emittance as a function of vertical chromaticity at vertical tune $\nu_y = 6.22$ for the SPEAR3 storage ring, simulation compared to theory.

$$\langle \mathcal{H}_c \rangle = \frac{\beta_y \chi^2 \bar{\eta}^2}{48} \csc^4 \pi\nu_y (2 + \cos 2\pi\nu_y) + \xi_y^2 \frac{\beta_y \chi^2 \pi^2 \sigma_\delta^2}{360} (120\beta_z^2 - 299\bar{\eta}^2 + 15\bar{\eta}^2 \csc^2 \pi\nu_y (7 + 30\csc^2 \pi\nu_y)) \csc^2 \pi\nu_y \quad (33)$$

The first term in Eq. (33) is the linear term originated from the coupling of the crab cavity. It is identical with the Eq. (76) in Ref. [7].

Using the same SPEAR3 parameters, with vertical beta function $\beta_y = 2.80$ m, momentum compaction $\alpha_c = 1.169 \times 10^{-3}$, bunch length $\sigma_z = 4.915$ mm, and other parameters as listed in Table I, the calculated vertical emittance is compared to the simulation in Fig. 3. The simulation and theoretic results agree reasonably well though small deviations are also found. It could be caused by other nonlinearities in the full ring (e.g., geometric effect from sextupoles), which are not accounted for the present model.

IV. CONCLUSION

In conclusion, we, for the first time, presented a case for which the storage ring equilibrium beam emittance depends on the lattice nonlinearity. In this case, the nonlinear longitudinal-vertical coupling due to crab cavities and the nonzero vertical chromaticity affects the excitation of the vertical eigenmode by photon emission and in turn the vertical emittance. This phenomenon was studied theoretically and by simulation. Analytic formulas for decoupling the longitudinal and vertical eigenmodes and the emittance dependence on chromaticity were derived. The simulation results were found to agree well with the predictions by the analytic formulas. The dependence of equilibrium emittance on lattice nonlinearity revealed in this study could enter future lattice design considerations and provide new ways for machine control.

ACKNOWLEDGMENTS

This was supported by the U.S. Department of Energy, Office of Science, Office of Basic Energy Sciences, under Contract No. DE-AC02-76SF00515.

[1] E. Courant and H. Snyder, Theory of the alternating-gradient synchrotron, Ann. Phys. (Paris) **3**, 1 (1958).
[2] M. Sands, Report No. SLAC Report SLAC-r-121, 1970.
[3] A. W. Chao, Evaluation of beam distribution parameters in an electron storage ring, J. Appl. Phys. **50**, 595 (1979).
[4] K. Ohmi, K. Hirata, and K. Oide, From the beam-envelope matrix to synchrotron-radiation integrals, Phys. Rev. E **49**, 751 (1994).
[5] A. Zholents, P. Heimann, M. Zolotorev, and J. Byrd, Generation of subpicosecond x-ray pulses using rf orbit deflection, Nucl. Instrum. Methods Phys. Res., Sect. A **425**, 385 (1999).
[6] A. Zholents, A new possibility for production of sub-picosecond x-ray pulses using a time dependent radio frequency orbit deflection, Nucl. Instrum. Methods Phys. Res., Sect. A **798**, 111 (2015).
[7] X. Huang, Coupled beam motion in a storage ring with crab cavities, Phys. Rev. Accel. Beams **19**, 024001 (2016).
[8] A. Bazzani, P. Mazzanti, G. Servizi, and G. Turchetti, Normal forms for hamiltonian maps and nonlinear effects in a particle accelerator, Nuovo Cimento B **102**, 51 (1988).
[9] D. Sagan and D. Rubin, Linear analysis of coupled lattices, Phys. Rev. ST Accel. Beams **2**, 074001 (1999).
[10] E. Forest, J. Math. Phys. (N.Y.) **31**, 1133 (1990).
[11] A. Terebilo, Accelerator modeling with Matlab Accelerator Toolbox, in *Proceedings of the Particle Accelerator Conference, Chicago, IL, 2001* (IEEE, New York, 2001), pp. 3203–3205.